Shale gas accumulation mechanism in the shallow burial depth: Insights from mechanical properties and methane adsorption capacity

Duo Wang
Institute of Geology and Geophysics, Chinese Academy of Sciences, Beijing, China
SINOPEC Petroleum Exploration and Production Research Institute, Beijing, China

Xiao Li
Institute of Geology and Geophysics, Chinese Academy of Sciences, Beijing, China

Hang Yuan
School of Geophysics and Information Technology, China University of Geosciences, Beijing, China

Guanfang Li
Institute of Geology and Geophysics, Chinese Academy of Sciences, Beijing, China

ABSTRACT: The shallow burial depth shale gas reservoirs have great significance for low-cost development. Petrophysical characteristics and methane adsorption capacity are fundamental factors that control shale gas enrichment. We investigated petrophysical characteristics and methane adsorption capacity based on lithology and burial depth. Several samples from reservoirs and sealing formation were analyzed to elucidate the enrichment mechanism, applying N_2 and CH_4 adsorption, petrophysical test, and micro CT scanning. The results indicate that the combination of high clay content calcareous siltstone and shale has obvious sealing capacity comparing to siliceous shale, and less fractures could be induced because of uplift. Besides, a shallow shale gas enrichment model was proposed, methane adsorption capacity is highly related to the burial depth, in the ultra-shallow depth (<700 m), a rapidly decreasing trend can be observed under a normal pressure condition, while there is no obvious decline of the adsorption capacity in the overpressure reservoirs.

Keywords: shallow shale gas; enrichment mechanism; petrophysical characteristics; methane adsorption.

1 INTRODUCTION

Since the successful hydraulic fracturing of shale gas in North America in the 1980s, the global energy landscape has witnessed a significant revolution with shale gas becoming a focal point and challenge in unconventional natural gas exploration(Li et al., 2023). Currently, China's exploration and development efforts primarily focus on deep- to ultra-deep natural gas fields within the depth range of 2000-4000 meters(Guo et al., 2023), while shallow shale gas reservoirs, located within depths shallower than 1500 meters, have been traditionally considered lacking in commercial viability due to factors such as low formation pressure coefficient, low total organic carbon (TOC) content, and significant structural disturbances. Notably, the Antrim Shale in Michigan represents the main shallow shale gas play in North America. However, in China, as shale gas resource exploration progresses in a more refined manner, commercially viable shallow shale gas reservoirs have been discovered in the Taiyang anticline area of Zhaotong, Yunnan Province, and the Xishui anticline area of Guizhou Province(Liang et al., 2023; Wang et al., 2022). Shallow shale gas

reservoirs offer advantages such as low development costs and rapid construction. Extensive research has already been conducted on the characteristics of deep to ultra-deep shale gas reservoirs, enrichment mechanisms(Jin et al., 2018), and key factors influencing production in the Sichuan Basin. It has been established that shale reservoirs with characteristics such as significant thickness, high TOC content, high porosity, high gas content, high silica content, and susceptibility to hydraulic fracturing form the foundation for shale gas enrichment and high productivity(Guo et al., 2023). Furthermore, many scholars have emphasized the importance of top and bottom sealing conditions and the strength of later-stage tectonic movements as crucial elements for shale gas accumulation. While the understanding and evaluation of shallow shale gas reservoirs in Xishui, Guizhou, provide valuable insights and references, the formation mechanisms and enrichment models for shallow shale gas remain subjects requiring further investigation. In this study, employing rock physics testing, gas adsorption analysis using CH_4 and N_2, and CT scanning, we systematically investigate the evolution of pore structure and methane adsorption capacity in shallow shale gas reservoirs. The research findings contribute to the evaluation and exploration of shallow shale gas resources.

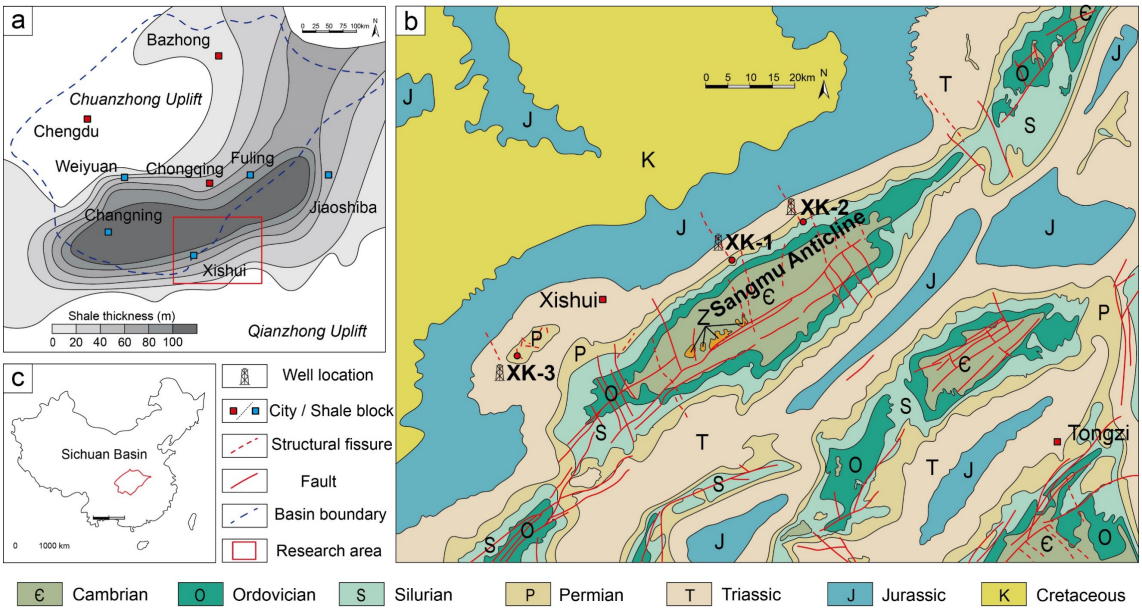

Figure 1. Isopach map of Longmaxi Formation in Sichuan Basin and location map of main shale blocks in Sichuan Basin (a), a geological map of regional tectonic units and shallow shale gas well location (b), the location map of Sichuan Basin in China (c).

2 GEOLOGICAL BACKGROUND

The Xishui shallow shale gas field is located at the intersection of the north-south and northeast-southwest structural belts in the southern part of Sichuan and northern part of Guizhou, adjacent to the Sichuan Basin in the north, the Qianzhong uplift in the south, and connected to the Jiangnan ancient landmass in the east. Geologically, it is positioned in the central part of the Yangtze platform. The research team conducted a series of scientific vertical drilling campaigns, including XK-1 (156 m), XK-2 (425 m), and XK-3 (704 m), in the northwestern flank of the Sangmu anticline in Xishui. The Sangmu anticline, approximately 70 km long and 15 km wide, trends in a NE-SW direction (Figure 1). It is the largest fold structure in the southern Sichuan and northern Guizhou region and exhibits a rhomboidal distribution pattern. The core of the anticline is characterized by two sets of nearly parallel main faults trending in the NE direction, with several minor faults and structural fractures branching off in the NW direction at both ends. The flanks of the anticline are characterized by the submergence of the Cambrian to Late Cretaceous strata, exhibiting an inclination of 15-30°. The Upper Ordovician Wufeng Formation-Lower Silurian Longmaxi Formation, with an average thickness of 30 m, is identified as a high organic matter reservoir interval. The formation pressure

coefficient is approximately 1.17, and the total organic carbon (TOC) content ranges from 1.25% to 7.26%. In-situ gas content measurements have reached a maximum of 6.01 m^3/t. Hydraulic fracturing was performed in the open-hole section of the Wufeng Formation-Longmaxi Formation in XK-3 well, yielding a shale gas flow rate of 4600 m^3/d.

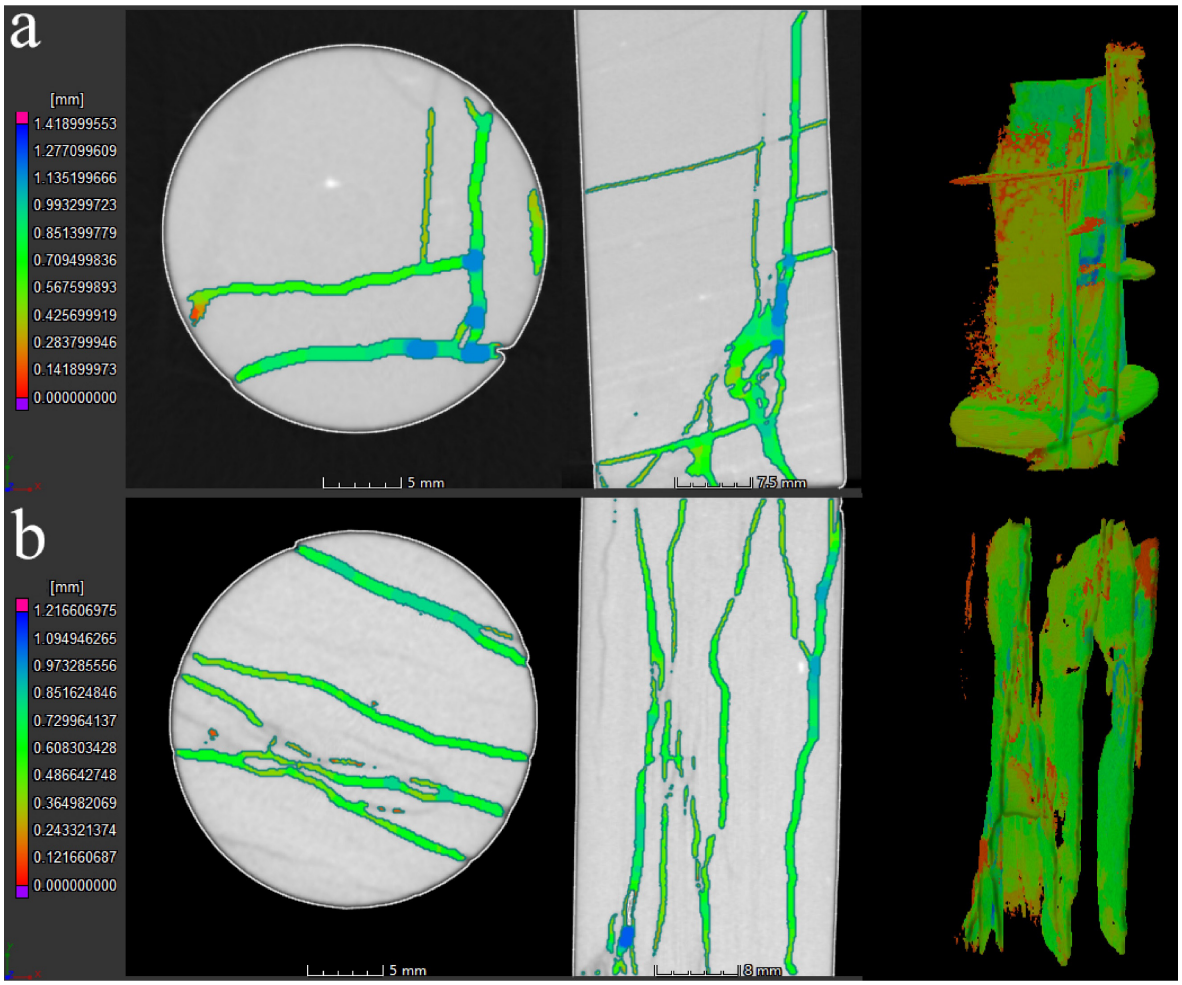

Figure 2. Compression failure modes of bedding horizontal shale samples (a), compressive failure modes of bedding vertical shale samples (b).

3 RESULTS AND DISCUSSION

3.1 Permeability and fracture propagation mode

Previous research has demonstrated the substantial effect of mineral structure on permeability, in particular the 40 times variation between vertical and parallel permeability due to the laminated structure of shale(Zhang et al., 2019). Based on pulse pressure testing, our research investigates the vertical and parallel permeability of the gas-bearing layer, the bottom sealing layer, and the top sealing layer. The average lateral permeability of the gas-bearing stratum, formed of organic-rich siliceous shale, was eight times greater than its vertical permeability, which measured 0.0923 md. Similar to the top sealing layer, the lower sealing layer, composed of organic-medium calcareous shale, has an average lateral permeability four times greater than its vertical permeability, measuring 0.2123 md. The top sealing layer, which consisted of organic-poor calcareous siltstone, had an average lateral permeability that was 2.33 times greater than its vertical permeability, measuring 0.0627 md. In addition, we conducted permeability tests on samples with visible fractures and found

that their permeability was two orders of magnitude more than that of those with no visible fractures. High lateral permeability can encourage bedding planes as major migration pathways in both reservoirs and sealing formations, according to these findings. However, tectonic activity-induced cracks can have a substantial effect on the migration of shale gas.

We analyzed the rock strength and fracture propagation characteristics of reservoirs and sealing layers under various stress circumstances. Despite the fact that the bedding dip angle in the research area spans from 1 to 10°, we did not evaluate its effect on rock strength because it has been thoroughly investigated. Fracture propagation of the bottom sealing layer, the gas-bearing layer, and the sealing layer is presented. The organic-rich siliceous shale gas-bearing layer has the highest siliceous content and a compressive strength of 150 MPa. The organic-medium calcareous shale of the Bottom sealing layer has a little lower strength of 180 MPa than the organic-poor calcareous siltstone of the top sealing layer (Figure 2). During fracture expansion, the gas-bearing layer tends to generate 1-2 main fractures and multiple secondary fractures due to a well-developed bedding fracture network, whereas the calcareous shale and calcareous siltstone of the sealing layer tend to generate a single main fracture along the principal stress direction. The exposed surface rock layers in the field confirms this mechanism of fracture rupture. The reservoir siliceous shale develops two sets of dominating joint planes, whereas the calcareous shale and calcareous siltstone of the sealing layer lack a major fracture network and only develop through faults or huge deposits. This suggests that vast calcareous shale and calcareous siltstone have a strong resistance to stress disturbance when subjected to tectonic uplift, due to their high clay mineral composition. According to our investigation, the compaction section and plasticity of these rocks during the stress-disturbance process are more pronounced.

3.2 Adsorption capacity evolution

The gas storage capacity of reservoirs is evaluated based on the Langmuir isotherm adsorption model (Eqs. 1) in academic research. This model effectively describes the methane adsorption behavior in the micro- and nano-pore structures of shale formations(Psarras et al., 2017). The parameters of this model mainly include the Langmuir pressure (V_L) and volume (P_L), which can be obtained through high-temperature and high-pressure methane adsorption experiments. However, during the early stages of reservoir development evaluation, it is challenging to acquire the parameters of the Langmuir model. In such cases, the establishment of empirical models for reservoir adsorption can quickly assess the changes in adsorption capacity in similar depositional environments.

Numerous scholars have found that the Langmuir pressure (V_L) is primarily influenced by the organic matter content and experimental temperature. Therefore, a multivariate linear regression can be used to establish the relationship between the total organic carbon (TOC), temperature (T), and VL. Additionally, there is an exponential correlation between the Langmuir pressure (P_L) and the experimental temperature (T). Thus, an empirical formula considering reservoir temperature and pressure conditions can be established to evaluate adsorption capacity. Furthermore, due to the correlation between burial depth and formation temperature and pressure (Eqs. 2), the variation in adsorption capacity with burial depth under overburden pressure (P_{OP}) and hydrostatic pressure (P_{HP}) conditions has been established based on well logging and basin simulation (Figure 3).

$$V = \frac{V_L P}{P_L + P} \tag{1}$$

$$V = \frac{[a_1 TOC + b_1 T + c_1] P_{OP/HP}}{a_2 e^{b_2 T} + P_{OP/HP}} \tag{2}$$

As shown in Figure 3a, the hydrostatic pressure model exhibits a slow incremental increase followed by a rapid decrease in adsorption capacity with decreasing burial depth, with a transition point ranging from 700 to 1300 meters. In the overburden pressure model, a significant decrease in adsorption capacity does not occur even in the ultra-shallow reservoirs (<700 meters). Figure 3b

illustrates the linearly increasing trend of adsorption capacity with increasing TOC, primarily due to higher TOC samples having more adsorption sites. Figure 3c compares the adsorption models calculated using empirical formulas with the measured values. The data for depths of 115-140 meters and 375-395 meters correspond to wells XK-1 and XK-2, respectively, which are considered normal-pressure shale gas reservoirs. Therefore, the hydrostatic pressure model fits the measured data well. The data for a depth range of 645-665 meters corresponds to well XK-3, which represents an overpressure shale gas reservoir. In this case, the overburden pressure model provides a good fit to the measured data.

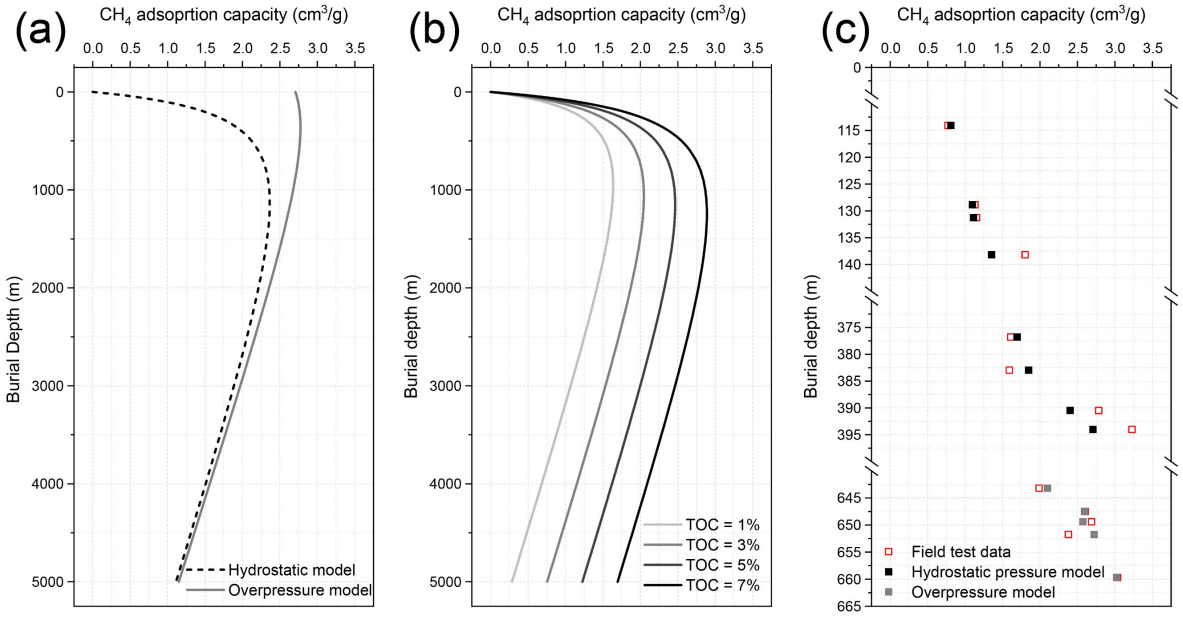

Figure 3. The adsorption capacity comparison of the hydrostatic model and overpressure model (a); The hydrostatic adsorption capacity evolution with increasing TOC content (b); The verification of the predicted model with the field desorption test data (c).

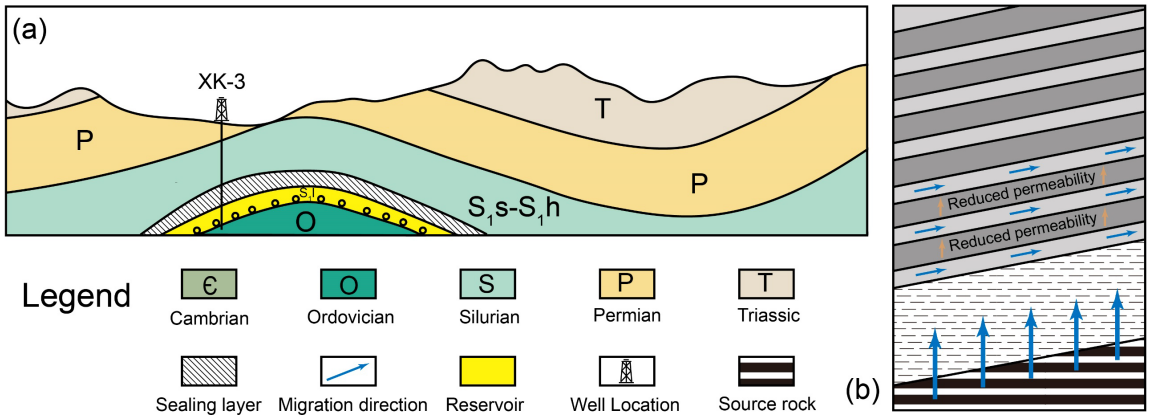

Figure 4. Schematic diagram of the geological section of Well XK-3 (a); Schematic diagram of gas dominant migration channel (b).

3.3 Enrichment mechanism of shallow shale gas

The high-yield enrichment of shallow shale gas reservoirs mainly includes two factors: firstly, the formation conditions of overpressure help to ensure that the reservoir has a high methane adsorption capacity (>2.0 m^3/t). Secondly, good preservation conditions are the main guarantee for enrichment

and high yield. As shown in Figure 4b, when the methane produced by the source rock migrates upward, the argillaceous shale of the sealing layer has a good sealing effect, while the high-density interbeds help to significantly reduce the upward escape of gas.

4 CONCLUSION

A geological model for shallow burial depth shale reservoirs was proposed based on the burial history, which can be used to reconstruct the evolution of methane adsorption capacity of both overpressure and hydrostatic model. A clear turning point of maximum adsorption volume can be found at a burial depth of approximately 700 m to 1300 m in normal pressure model, while there could be high adsorption capacity if the reservoirs is over pressured in the ultra-shallow depth (< 700 m).

The enrichment mechanism of shallow burial depth shale gas reservoirs is including two key factors, which is the sealing formation consisting with high clay content calcareous siltstone and shale. And formation overpressure is the prerequisite for shallow shale gas to have high adsorbed gas content, and it is also the guarantee for long-term stable production capacity.

ACKNOWLEDGEMENTS

This work is supported by the National Natural Science Foundation of China (Grant No. 42090023).

REFERENCES

Guo, X., Hu, D., Shu, Z., Li, Y., Zheng, A., Wei, X., Ni, K., Zhao, P., & Cai, J. (2023). Exploration, development, and construction in the Fuling national shale gas demonstration area in Chongqing: Progress and prospects. *Natural Gas Industry B*.

Jin, Z., Nie, H., Liu, Q., Zhao, J., & Jiang, T. (2018). Source and seal coupling mechanism for shale gas enrichment in upper Ordovician Wufeng Formation-Lower Silurian Longmaxi Formation in Sichuan Basin and its periphery. *Marine and Petroleum Geology*, *97*, 78-93.

Li, G., Jin, Z., Li, X., Zhang, P., Liang, X., Zhang, R., Li, C., Wang, D., & Hu, Y. (2023). Shallow burial shale gas accumulation pattern of the Wufeng–Longmaxi Formations in the northern Guizhou area, western Yangtze platform. *Geoenergy Science and Engineering*, *225*, 211683.

Liang, X., Wang, W., Li, Z., Zhu, D., Xu, J., Zhang, Z., Zhang, Z., Luo, Y., & Yuan, X. (2023). Exploration and development in the Zhaotong national shale gas demonstration area: Progress and prospects. *Natural Gas Industry B*.

Psarras, P., Holmes, R., Vishal, V., & Wilcox, J. (2017). Methane and CO2 adsorption capacities of kerogen in the Eagle Ford shale from molecular simulation. *Accounts of chemical research*, *50*(8), 1818-1828.

Wang, D., Li, X., Li, G., Mao, T., & Zheng, B. (2022). The Characterization of Shale Differences Based on Petrophysical Properties and Pore Structure: A Case Study of the Longmaxi Formation in Northern Guizhou Province and the Yanchang Formation in the Ordos Basin. *Applied Sciences*, *12*(11), 5303.

Zhang, K., Song, Y., Jiang, S., Jiang, Z., Jia, C., Huang, Y., Liu, X., Wen, M., Wang, X., & Li, X. (2019). Shale gas accumulation mechanism in a syncline setting based on multiple geological factors: An example of southern Sichuan and the Xiuwu Basin in the Yangtze Region. *Fuel*, *241*, 468-476.